Eur. Phys. J. B **53**, 67–76 (2006)
DOI: 10.1140/epjb/e2006-00348-9

THE EUROPEAN PHYSICAL JOURNAL B

Statistical verification of crystallization in hard sphere packings under densification

K. Lochmann[1], A. Anikeenko[2], A. Elsner[3], N. Medvedev[2], and D. Stoyan[1,a]

[1] Institute of Stochastics, TU Bergakademie Freiberg, 09596 Freiberg, Germany
[2] Institute of Chemical Kinetics and Combustion SB RAS, Institutskaya 3, 630090 Novosibirsk, Russia
[3] Institute for Solid State and Materials Research, IFW Dresden, P.O. Box 270116, 01171 Dresden, Germany

Received 25 April 2006 / Received in final form 5 July 2006
Published online 7 September 2006 –

Abstract. The performance of various structure characteristics in the task of indicating structural peculiarities in packings of hard spheres is investigated. Various characteristics based on Voronoi polyhedra, spherical harmonics, and Delaunay simplices are considered together with the pair correlation function and the mean number of r-close triples. They are applied to a set of hard sphere packings of density ϕ from 0.62 to 0.72. It turns out that all used structure characteristics are able to indicate changes of order from non-crystalline to crystalline packings. However, not all of them are sensitive enough to indicate different stages of structure transformation under densification. The characteristics based on Delaunay simplices turn out to be the most sensitive for this purpose. For the models considered three principal structure classes are found: packings of densities lower than the known critical value 0.64 showing a non-crystalline behavior; packings with considerable crystalline regions for ϕ up to 0.66–0.67; rather complete crystals although with numerous defects for ϕ above 0.67.

PACS. 61.43.-j Disordered solids – 61.43.Bn Structural modeling: serial-addition models, computer simulation

1 Introduction

Packings of identical hard spheres are useful models in the study of the structure of diverse systems in physics, chemistry and engineering. They approximate well the structure of atomic and granular systems. Moreover, they are able to reproduce the liquid-to-solid phase transition, including both freezing of liquid to crystal and 'glass transition' [1–5]. Hard sphere systems give a striking physical example illustrating that the structure of atomic systems is governed mainly by short-range repulsion and, ultimately, by geometrical properties of spheres in 3D-space.

The structure and degree of disorder in hard spheres depend heavily on the density or packing fraction ϕ. At $\phi = 0.494$ the liquid phase of hard sphere systems becomes non-stable. With increasing density crystallization may begin, or such a system may become a supercooled liquid and then, somewhere at $\phi = 0.56$ [6], take a solid amorphous state. The disordered (non-crystalline) packing of hard spheres has a limited density around 0.64. This is proven well both experimentally [7–11] and by computer simulation [12–15]. The densest hard sphere systems are crystalline, namely fcc and hcp (both with $\phi = 0.7405$), however a 'stable' crystalline phase exists until $\phi = 0.545$ (melting point).

The investigation of the structure of simulated models of atomic systems stimulated the development of new statistical methods, additionally to the classical use of pair correlation function and structure factor known in physics of liquids. These methods are based on quite different concepts. One of them uses tessellations, starting with the work by Bernal on Voronoi polyhedra [7,16]. Metrical and topological parameters of the Voronoi polyhedra around atoms reflect geometrical properties of the close neighborhoods of atoms in the system. In particular, the number of polyhedra faces indicates the quantity of 'natural' neighbors, and the volume of Voronoi polyhedra defines a 'local density' [3,17,18]. Finney [19] coined in this context the term 'polyhedral statistics'. Also the Delaunay tessellation, which is dual to the Voronoi tessellation, turned out to be a valuable statistical tool [20–22]. A Delaunay simplex is defined by a quadruple of 'mutually closest' atoms. Such quadruples of atoms represent 'bricks' which compose the atomic system; therefore their analysis is particularly useful for structure investigation. The simplex shapes play an important role in structure characterization, for which various measures can be used [21]. In particular, they can be used to select simplices of a shape close to that of a perfect tetrahedron. The spatial distribution of such simplices inside an atomic system gives valuable structural information [22]. The use of Delaunay simplices, Voronoi

[a] e-mail: stoyan@orion.hrz.tu-freiberg.de

polyhedra and the corresponding tessellations for structure investigations is known as the 'Voronoi-Delaunay method', which is applied in many fields of science [23,24].

Another approach for studying the structure of atomic systems uses the bond-orientational order characteristic Q_6 [25]. The idea is to decompose the vectors directed from an atom to its neighbors into spherical harmonics. The corresponding coefficients Q_{lm} depend on the arrangement of the neighbors and thus specific invariants of them (in particular, Q_4, Q_6, W_6 [4,25–29]) can be used to characterize the structure of the neighborhoods. Q_6 is used in a local and global version [28,30].

Finally, two further useful order metrics appeared in the literature, namely the 'translational order characteristic' T [29,31] and, going beyond second-order characterization, a third-order characteristic $T_3(r)$ proposed in [32], which will both be explained below.

The present paper has two aims: to show structural differences in disordered packings of identical spheres of different packing density, and to compare the ability of the various statistical characteristics to indicate the occasionally rather fine structural differences in these packings.

The packings examined here have densities between 0.62–0.72. We characterize our packings as 'maximally disordered' for a given density. It is not very clear how to formulate this condition mathematically, however intuitively its physical meaning is understandable. Indeed, structures of packings of a given density can be very diverse. It is known that a packing may contain crystalline nuclei starting from a density of 0.495. On the other hand it can be completely non-crystalline up to $\phi \approx 0.64$. The structure of a packing depends on the protocol of the simulation; both on the algorithm and on the parameters of the given algorithm (see e.g. [33,34]). A long evolution and perceptible amount of free volume enable the appearance of crystalline nuclei, while a fast quenching or densification of an initial random configuration of spheres results in a 'jammed' disordered packing. Our packings with density up to $\phi \approx 0.64$ do not contain any recognizable crystalline nuclei or aggregates of any other specific symmetry. (They could be clearly detected by the pair correlation function, or, with more precision, using spherical harmonics [10] or shape analysis of Delaunay simplices [35,36].) In this meaning these packings can be called maximally disordered. Note that such packings are obtained very easily in experiments [10]. The packings with higher density cannot be created without crystalline nuclei. In this case we can speak about a maximal disorder because we did not go far (in configurational space) from the obtained non-crystalline packings using our procedure of densification, see Section 2. The crystalline nuclei which spring up in our packings on the interval 0.64–0.66 are randomly distributed. The more dense packings (denser then 0.67) obviously represent a 'total' crystalline structure, and the disorder in this models is realized by numerous defects in the crystal. We think that maximal disorder at these high densities can only be realized in this way.

Digressing from physical processes resulting in such packings and from computational algorithms of generation, our packings can be considered as sets of 'points' in some configurational space (each point represents a concrete configuration of non-overlapping spheres in space), and we use them to demonstrate a feasible disorder for a given density.

Clearly, different structural characteristics indicate different properties of packing structures. In particular, characteristics determined by many atoms such as Voronoi polyhedra and spherical harmonics invariants, which are based on about 15 neighbor atoms, are hardly able to detect small crystalline nuclei at the beginning of crystallization. In contrast, Delaunay simplices seem to be better adapted to the problem of finding fine structural peculiarities, since they are defined by quadruples of atoms.

The performance of these and other structure characteristics is systematically compared. By the way, it is difficult to order the various characteristics systematically. We consider here four groups, where the first contains mainly characteristics that consider the packing from the standpoint of a single atom. The other three groups are related to the number of atoms directly involved in the definition: two-pair correlation function, three-triplet correlation and four-Delaunay simplex.

2 Generation of sphere packings

The hard-sphere packings studied in this paper were generated using the so-called force-biased algorithm [15,37], which belongs to the family of so-called 'collective rearrangement' algorithms. It is based on the classical algorithm used in [12,38].

The initial configuration of the algorithm is a set of N spheres with random centers uniformly distributed in a cubic container. Overlappings are permitted. While the number of spheres is fixed, the algorithm attempts to reduce overlaps between spheres by shifting overlapping spheres and gradual shrinking of the radii. Periodic boundary conditions are used.

An important element of the algorithm is a 'repulsion force', F_{ij}, between each pair (i,j) of overlapping spheres, which determines the extent of the shifts. It controls heavily the efficiency of the algorithm, see [15]. In every step, for all spheres these shifts and a shrinking operation, which reduces all radii by the same factor, are carried out. This is continued until all overlappings vanish.

This algorithm leads to packings of ϕ around 0.66. To obtain packings of higher densities, the result of an earlier run of the algorithm is used as a starting configuration, where the corresponding diameters are enlarged so that new overlappings may appear. This procedure can be repeated several times.

All packings discussed in this paper consist of 10 000 spheres, a size which turned out to be large enough for our statistical investigations. For statistical purposes for each density ϕ several independent packings were generated; ten for $\phi < 0.7$, as we are mainly interested in structural changes happening between $\phi = 0.64$ and 0.7, and three for higher densities.

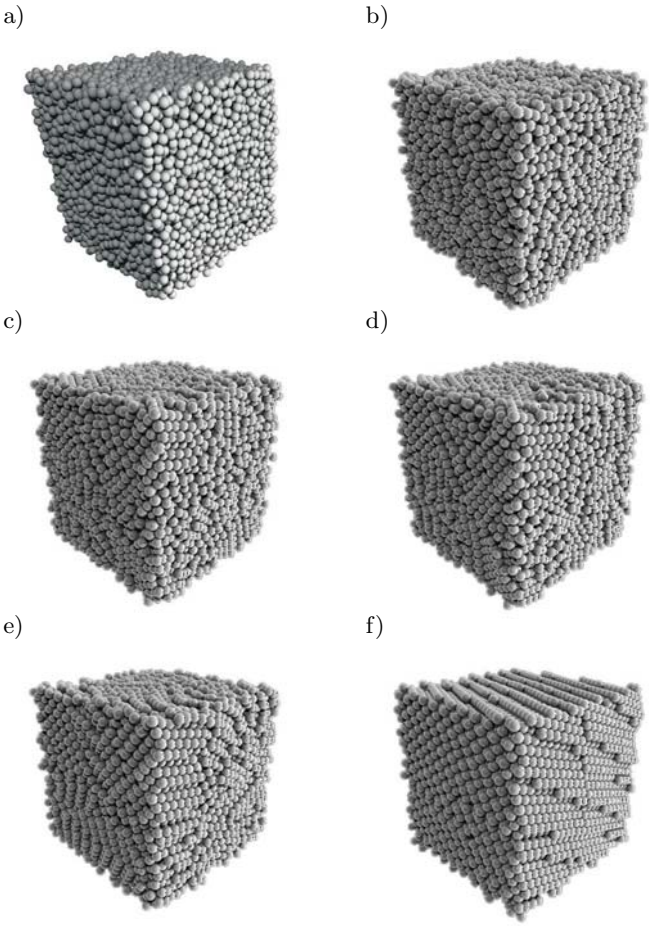

Fig. 1. A series of monosize hard-sphere packings with different densities: (a) 0.64; (b) 0.65; (c) 0.654; (d) 0.66; (e) 0.67; (f) 0.71. Each packing consists of 10000 spheres. The order in the packings increases with growing density.

Figure 1 shows a series of packings with different densities. The sample with density $\phi = 0.64$ looks like a completely disordered packing. The packing with $\phi = 0.65$ also looks disordered, but a few lineal rows of spheres can be recognized. However, a packing with $\phi = 0.654$ demonstrates clear crystalline regions, which becomes pronounced at $\phi = 0.66$. The packings at the bottom present completely crystalline samples. At $\phi = 0.67$ there are still a lot of defects, but at $\phi = 0.70$ an almost perfect dense crystalline structure can be observed. Thus, one can see that the more principal structural changes seem to take place in the rather narrow interval 0.64–0.66.

The question is how robust the structural changes of the packings are with respect to changes in the algorithm. To test this we generated models of 10 000 spheres of packing densities from 0.60 to 0.66 using a modified Lubachevsky-Stillinger algorithm [39]. This algorithm realizes Newtonian dynamics of hard spheres together with a gradual growth of their radii. Thus it is in some sense dual to the force-biased algorithm, where the radii are reduced. To get packings with 'a maximal disorder' (see Sect. 1), we chose a relatively high rate of growth of sphere radii; to obtain higher densities the rate of radius growth should be lower. A random configuration of non-overlapping spheres was used as initial configuration for each run. As result we obtained packings whose structure is statistically identical to the structure of packings used in this paper for the same packing fractions. Note that it was found that, if we choose slow growth of sphere radii in the Lubachevsky-Stillinger algorithm, small crystalline nuclei already appear in packings with rather low density, in particular from a density of 0.62.

3 Scalar order metrics

A famous measure of disorder in sphere packings is the *bond-orientational order characteristic* Q_6 [3,25,28,30,40–42]. It is applied in two forms. In the *global* version the whole network of all nearest neighbor bonds (defined by means of the Voronoi tessellation) is used,

$$Q_{6,global} = \left(\frac{4\pi}{13} \sum_{m=-6}^{6} \left| \frac{1}{N_b} \sum_{i=1}^{N_b} Y_{6m}(\theta_i, \varphi_i) \right|^2 \right)^{\frac{1}{2}}, \quad (1)$$

where N_b denotes the total number of bonds in the packing and $Y_{6m}(\theta_i, \varphi_i)$ are the spherical harmonics, with θ_i and φ_i being the polar and azimuthal angles of bond i. In this way a single number characterizes a whole packing.

In a perfect crystal these bonds have well-defined directions, which persist over macroscopic distances. Therefore it is natural that $Q_{6,global}$ takes large values if crystalline structures are present in the packing and reaches its maximum for the perfect fcc crystal, which is 0.57452, as stated e.g. in [40]. Below the behavior of $Q_{6,global}$ is shown in comparison with another order metric.

The *local* bond-orientational order characteristic $Q_{6,local}$ [3,26,28,30,41,42] for a single sphere is defined as

$$Q_{6,local} = \left(\frac{4\pi}{13} \sum_{m=-6}^{6} \left| \frac{1}{n_b} \sum_{i=1}^{n_b} Y_{6m}(\theta_i, \varphi_i) \right|^2 \right)^{\frac{1}{2}}, \quad (2)$$

where n_b is the number of nearest neighbors of the sphere considered and θ_i and φ_i are the polar and azimuthal angles of bond i of the sphere. The corresponding mean for the whole packing $\overline{Q}_{6,local}$ is the next disorder measure; since $Q_{6,global}$ and $\overline{Q}_{6,local}$ differ in the averaging procedure, they yield different numerical values. Below the behavior of $\overline{Q}_{6,local}$ is discussed in comparison with another order metric.

The quantity $\overline{Q}_{6,local}$ can be interpreted as the mean value of the random variable $Q_{6,local}$ associated with the spheres. This leads to the idea to consider also other aspects of the distribution of $Q_{6,local}$. While below the variance of $Q_{6,local}$ is discussed in comparison with the variance of another characteristic, Figure 2 presents the probability distributions of $Q_{6,local}$ for different values of ϕ. It shows that for the considered packings with densities around 0.7 a shoulder appears in addition to the main

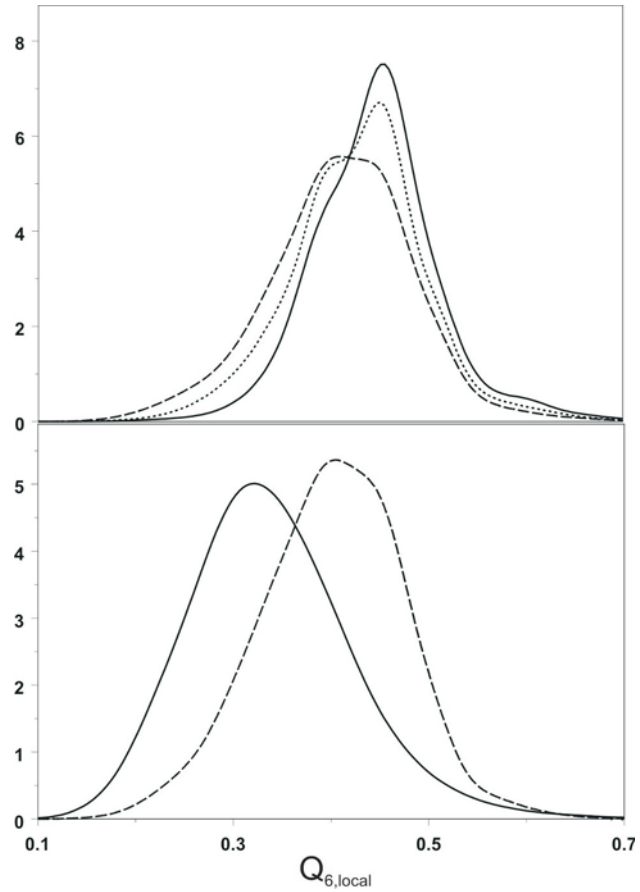

Fig. 2. Distributions of $Q_{6,local}$ under densification of hard sphere packings: bottom — 0.62 (—), 0.67 (– – –); top — 0.68 (– – –), 0.7 (- - -), 0.72 (—). While all distributions look like Gaussian distributions with increasing mean, around $\phi = 0.7$ there is an anomaly with a shoulder.

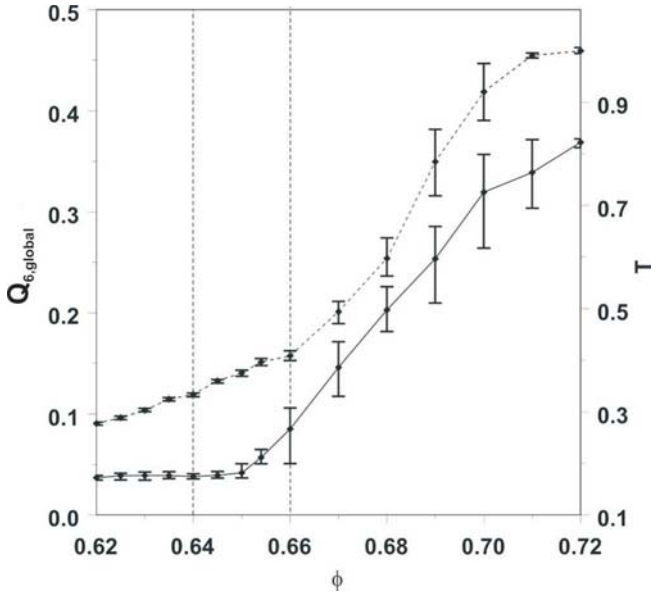

Fig. 3. Development of $Q_{6,global}$ (—) and T (– – –) under densification of hard sphere packings. The points represent the mean values for each density.

peak. This indicates a structural change at this density, related to the appearance of large crystalline regions, where both fcc and hcp structures may appear. Interestingly, this shoulder is transient, it vanishes with ongoing densification, in which a uniform crystalline structure develops, presumably fcc. Furthermore, the dispersion of the distributions clearly decreases while the mean increases with increasing ϕ.

Another well-known order metric is the *translational order characteristic* T introduced by Torquato et al. [43]. It measures the degree of spatial order in a hard sphere system relative to the perfect fcc structure [30,40,44]. T compares the mean occupation of thin shells concentric with each sphere to the mean occupation of the same shells in the fcc structure and in an ideal gas:

$$T = \left| \frac{\sum_{i=1}^{N_s} (n_i - n_i^{ideal})}{\sum_{i=1}^{N_s} (n_i^{fcc} - n_i^{ideal})} \right|. \quad (3)$$

Here n_i is the occupancy of the ith shell averaged over all spheres in the system and N_s the number of shells. n_i^{ideal} and n_i^{fcc} are the corresponding mean shell occupation numbers for an ideal gas and the fcc lattice, respectively. The positions and the width ε of shells are specified so that they correspond to the successive neighbor shells of the fcc lattice. As in [40] the first seven neighbor shells were considered in this paper, using a shell width $\varepsilon = 0.196$. By the way, it is easy to show that T is a second-order characteristic closely related to Ripley's K-function, which is an integrated form of the pair correlation function.

The performance of $Q_{6,global}$ and T for the analyzed hard sphere packings is shown in Figure 3. There is a continuous rising of T with ongoing densification with a steep increase at ϕ around 0.68. That means, T is able to detect 'good' crystals, but is not sensitive to the structural changes between $\phi = 0.64$ and 0.66. In contrast, $Q_{6,global}$ seems to perform better in the task of identifying and proving a beginning of crystallization since it changes its behavior after $\phi = 0.65$ greatly.

A different approach of structure characterization from the standpoint of single atoms is based on the Voronoi tessellation, which is widely used in the study of the geometrical arrangement of the hard spheres in packings (see e.g. [3,7,17,18,45]). It divides the space into convex polyhedral cells, where each cell contains exactly one sphere. Characteristics of Voronoi tessellations [23,24,44,46] which are useful for the comparison of sphere packings are the probabilities $p(f)$ of f-faceted cells and the mean number of faces $\langle f \rangle$ per cell, which also represents the mean number of neighbors of a sphere.

Figure 4 shows the probability distributions of the number of faces at different densities. Obviously the dispersion decreases with increasing ϕ, indicating the increasing degree of order in the packings. However, the

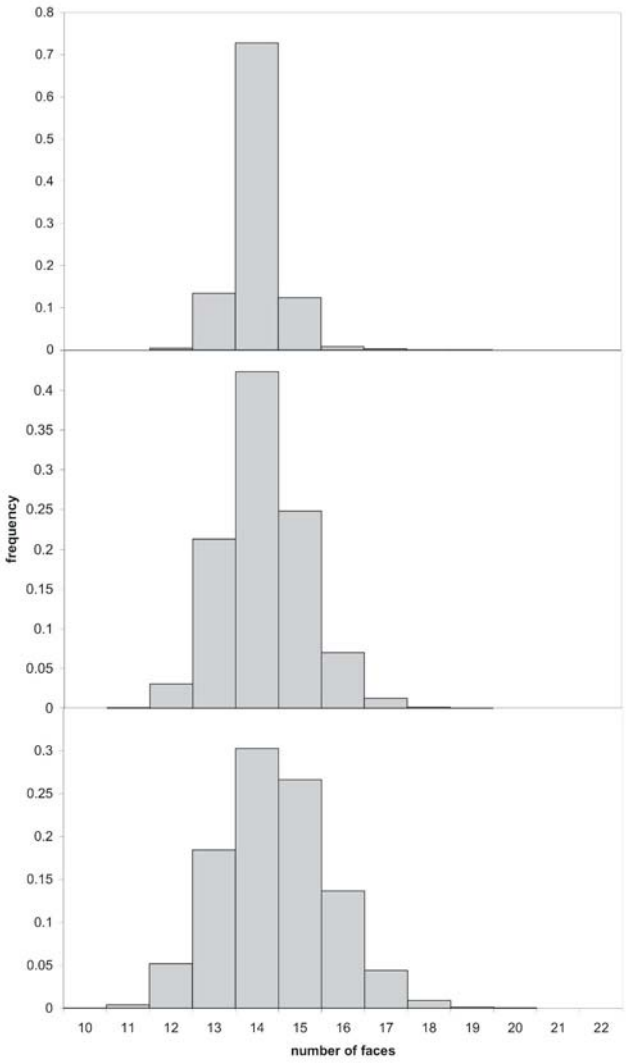

Fig. 4. Distributions of the number of faces per Voronoi cell for sphere packings with densities 0.62 (bottom), 0.654 and 0.72 (top). While the mean is nearly fixed, the variability decreases with increasing ϕ.

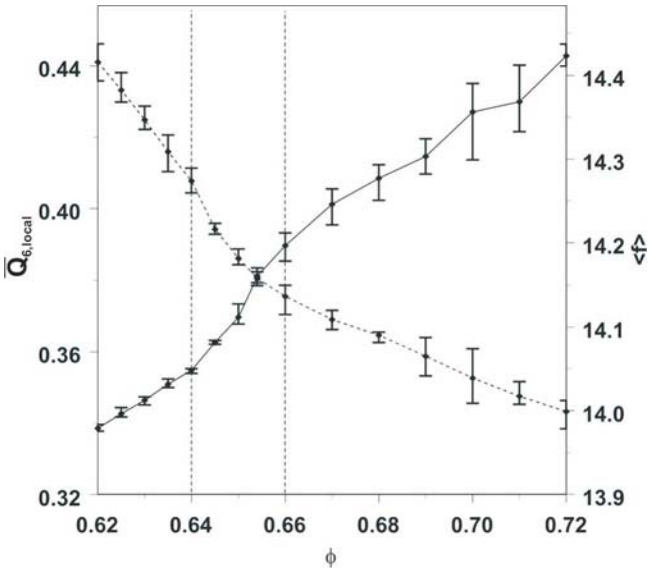

Fig. 5. Development of the local bond-orientational order characteristic $\overline{Q}_{6,local}$ (—) and of the mean number of faces per Voronoi cell $\langle f \rangle$ (– – –) during the densification of hard sphere packings.

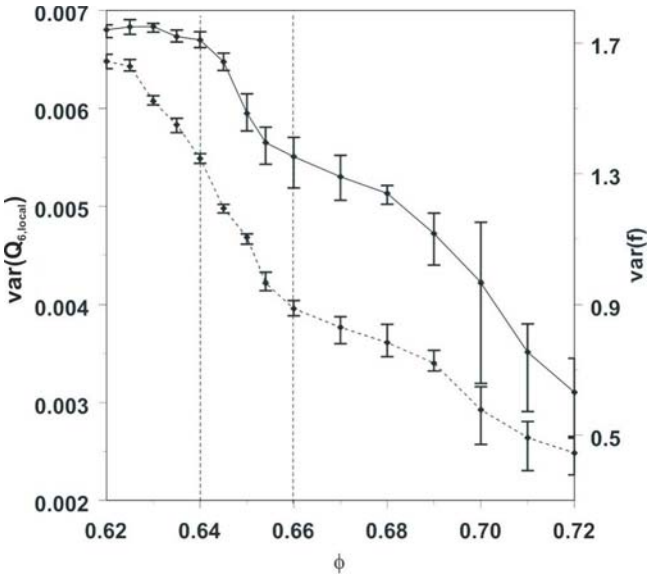

Fig. 6. Development of the variances of the local bond-orientational order $Q_{6,local}$ (—) and the number of faces per Voronoi cell f (– – –) at the densification of hard sphere packings. Both curves show a cusp point in the ϕ-interval 0.64–0.66.

distributions are not very sensitive to densification and hardly indicate structural changes.

While in Figures 3 and 4 probability distributions are compared, Figure 5 demonstrates the development of the mean $\overline{Q}_{6,local}$ and the mean number of faces $\langle f \rangle$ at the densification of sphere packings. It shows a continuous rising of $\overline{Q}_{6,local}$, while the mean number of faces per Voronoi cell decreases with increasing density, converging towards 14, the value for an fcc system. Both curves are nearly linear and do not indicate abrupt structural changes like a beginning of crystallization. In particular, no peculiarities can be observed at ϕ between 0.64 and 0.66.

A similar behavior was observed for the number of contacts between spheres: the mean number of contacts increases nearly linearly.

In addition to the mean value considered above, also other statistical characteristics of the distributions of $Q_{6,local}$ and f can be considered, e.g. their variance. For both the variance is decreasing with increasing ϕ, as shown in Figure 6. While for the variance of f no abrupt changes can be found, the variance of $Q_{6,local}$ has a steep descent at densities larger than 0.65, which may indicate structural changes.

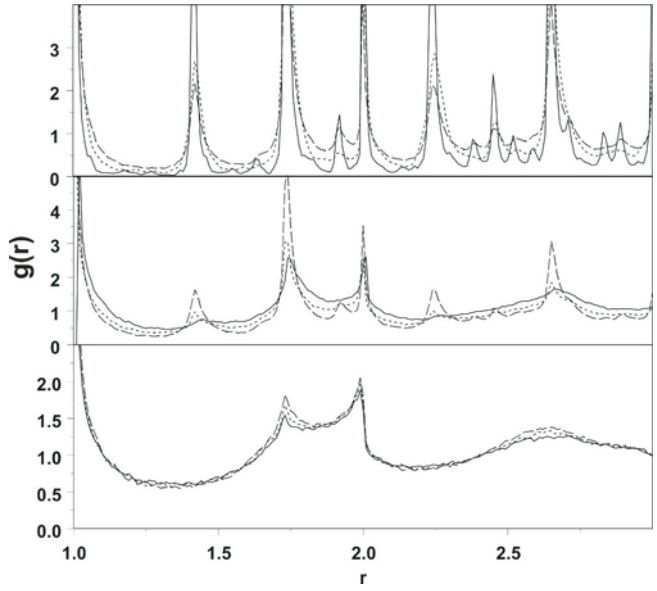

Fig. 7. Pair correlation function at different densities: bottom — 0.62 (—), 0.63 (- - -), 0.64 (– – –), middle — 0.654 (—), 0.66 (- - -), 0.67 (– – –); top — 0.68 (– – –), 0.7 (- - -), 0.72 (—). The small peak at $r = \sqrt{2}$ for $\phi = 0.66$ indicates structural changes in the packing.

4 Pair correlation function

A classical approach to analyze hard sphere packings is the use of higher-order characteristics for the point process of sphere centers. To this class belongs the pair correlation function $g(r)$ (or radial distribution function) [44], which is the most popular second-order characteristic in physical applications and usually more informative than scalar characteristics. It is able to indicate structural changes by small shoulders or maxima [47].

Figure 7 presents the pair correlation functions for three groups of hard sphere packings, representing disordered packings, packings with some crystal nuclei and crystalline structures, respectively. Here clear differences between the three groups of packings can be recognized. In the group of packings where crystallization starts a peak at $r = \sqrt{2}$ becomes slightly visible, which is an indicator of local crystalline order. This peak and other crystal-related peaks become still clearer with ongoing densification and are very pronounced at densities higher than 0.67. Thus the pair correlation function is obviously sensitive to structural changes in hard sphere packings going from disordered to ordered phase.

5 Triplet correlation

Now a third-order metric $T_3(r)$ is considered, which was introduced by Schladitz & Baddeley [32]. It results from integration of the well-known three-particle correlation function (see e.g. [44]), which itself is too complex for practical statistical applications. The characteristic $T_3(r)$ might be called *mean number of r-close triples*. For a packing of N hard spheres in the volume V, $T_3(r)$ is the mean

$$T_3(r) = \frac{1}{2\lambda^2}\frac{1}{N}\sum_{i=1}^{N} p_i(r), \tag{4}$$

where $p_i(r)$ is the number of pairs of sphere centers of distance smaller than r within the test sphere of radius r centered at the center x_i of the i-th sphere of the packing; in these pairs x_i is not included. For r a bit larger than 1, $T_3(r)$ describes the appearance of triples of contacting spheres, while $T_3(r) = 0$ for $r < 1$, because in a sphere of diameter smaller than 1 there cannot be other spheres of diameter 1. For larger r $T_3(r)$ is increasing and for a crystalline lattice structure it has jumps at the characteristic inter-point distances for fcc structures, namely at $r = 1, \sqrt{2}, \sqrt{3}, 2$ and so on. Nevertheless, by definition $T_3(r)$ is not directly related to some crystalline lattice. Methods for the estimation of $T_3(r)$ are described in [32]. For our calculations the so-called translation correction method was used.

Figure 8 shows $T_3(r)$ for three classes of packings. There is a completely different behavior of $T_3(r)$ for sphere packings with low and high density. For low density packings a nearly parabolical increase of $T_3(r)$ can be observed with increasing r, while for high densities jumps appear. This happens, as Figure 8 shows, not only for high density systems (0.68 and higher), but the first development in this direction can already be recognized at systems with $\phi = 0.654$, which indicates presence of crystal nuclei in the packings.

To compare $T_3(r)$ to scalar order characteristics it is helpful to consider its values at special distances r. An interesting behavior can be expected for $r = 1, \sqrt{2}, \sqrt{3}, 2$ and so on. However, numerical effects in the simulated packings make the choice of these values unattractive, but somewhat larger r's are useful. Therefore $T_3(1.1)$ and $T_3(1.5)$ are used.

As Figure 9 shows, $T_3(1.1)$ increases continuously, since with increasing ϕ the number of triples of contacting spheres increases. At $\phi = 0.65$ there is a sharp bend and a faster increase starts. For $T_3(1.5)$ even a slight decrease is visible, but then a still sharper bend is observed. This more sensitive reaction to structural changes is due to the fact that triples of spheres with distances up to $\sqrt{2}$ are bound to crystalline structures and rarely appear by chance.

6 Analysis of Delaunay simplices-quadruple correlation

6.1 Tetrahedricity and quartoctahedricity

While the Voronoi tessellation has proved to be a useful tool in the investigation of hard sphere packings, some disadvantages must be noted: each sphere has many neighbors in the Voronoi sense, such that the strength of influence of any particular sphere is unclear. Furthermore

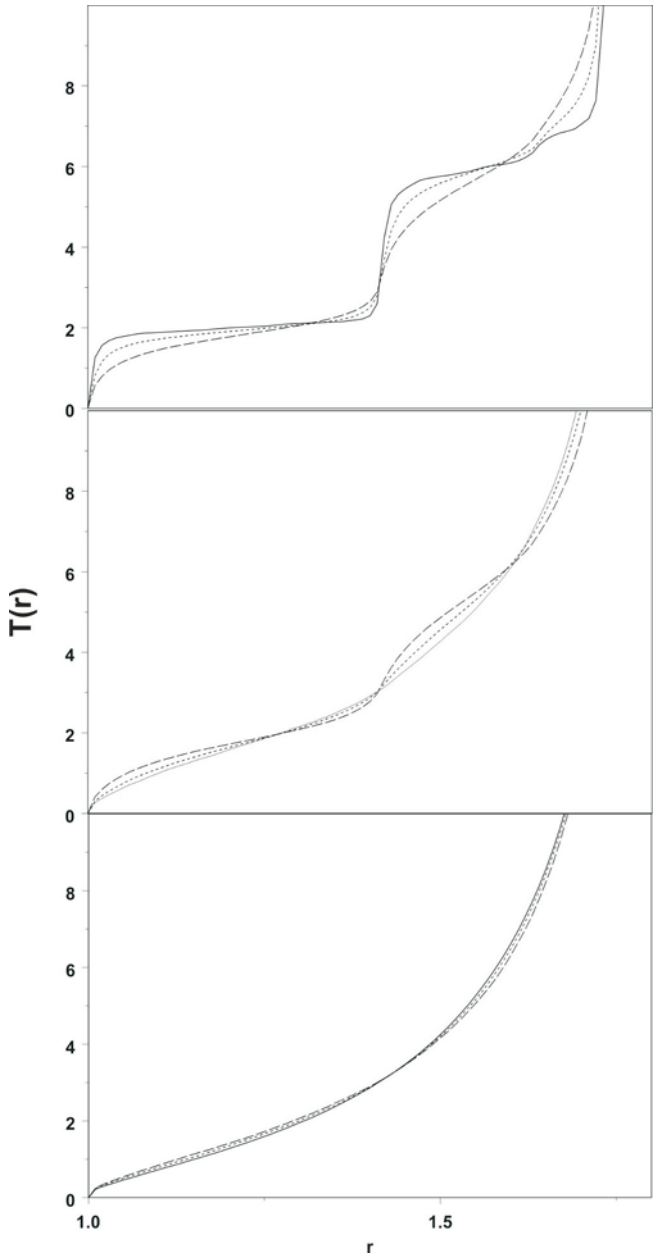

Fig. 8. The third-order characteristic $T_3(r)$ for sphere packings with densities between 0.62 and 0.72: bottom — 0.62 (—), 0.63 (- - -), 0.64 (– – –), middle — 0.654 (—), 0.66 (- - -), 0.67 (– – –); top — 0.68 (– – –), 0.7 (- - -), 0.72 (—). Already for $\phi = 0.654$ the curve shape changes from parabolic to stepwise.

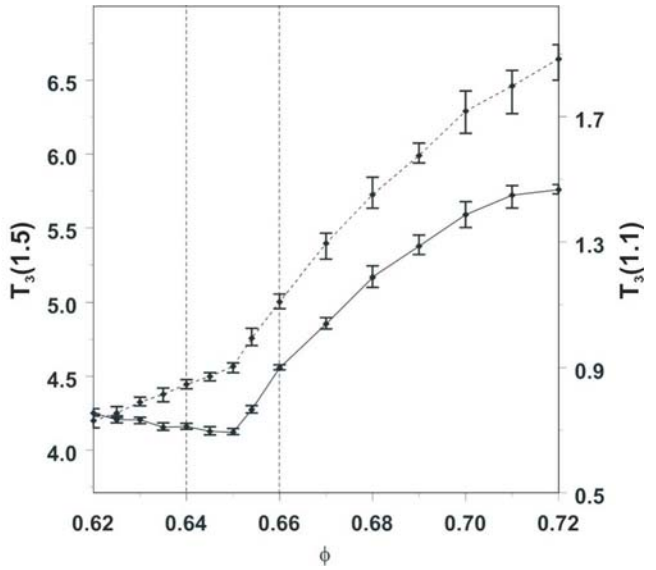

Fig. 9. Development of $T_3(1.5)$ (—) and $T_3(1.1)$ (– – –) with increasing density. Both functions have a cusp point in the interval 0.64–0.66 for ϕ, which indicates structural changes in the packings.

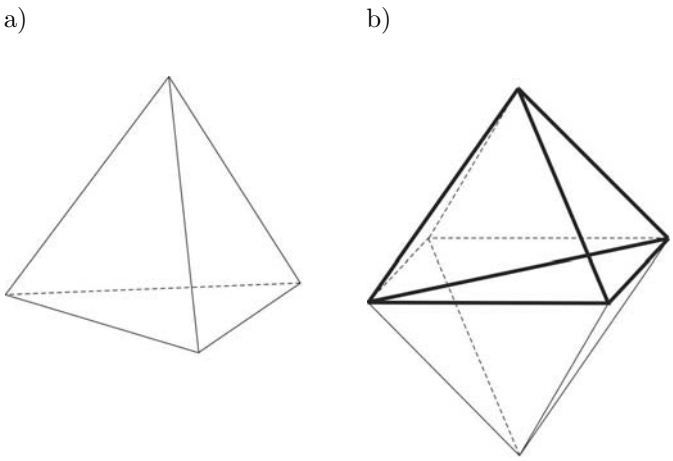

Fig. 10. Tetrahedra in crystalline packings: (a) perfect tetrahedron; (b) octahedron and quartoctahedron (bold).

the shape and topological characteristics of the Voronoi cells vary, e.g. the number of faces fluctuates. This has led to the idea to use its dual tessellation, the Delaunay tessellation. The edges of its cells connect those pairs of sphere centers whose Voronoi polyhedra share a common face. The cells, called Delaunay simplices, are tetrahedra having the centers of four neighboring spheres as vertices and have the property that no sphere centers are situated inside their circumscribed spheres. Thus, the Delaunay simplices compose the empty interstitial space in a hard sphere packing. They are related to exactly four neighboring spheres and so of a clear local character. As the Delaunay simplices are always tetrahedra, shape measurement and comparison is easy.

According to [21,22,48] in crystalline fcc and hcp structures only three typical forms of Delaunay simplices are possible: perfect tetrahedra, quartoctahedra (quarters of octahedra) and (flat) squares, as shown in Figure 10. Therefore the appearance of Delaunay simplices of these shapes in a hard sphere packing indicates the existence of crystalline parts.

Based on these ideas, in [23] simplex shape characteristics using the lengths of simplex edges were introduced. They exploit the fact that perfect tetrahedra and

quartoctahedra have typical edge length proportions, which can be used to define simplices of these shapes.

In a perfect tetrahedron all six edges have the same length. As this is only valid for perfect tetrahedra, a simplex fulfilling this condition must be a perfect tetrahedron. Consequently, in [21] the measure for tetrahedricity (**T**) of a simplex is defined as

$$\mathbf{T} = \frac{\sum_{i<j}(e_i - e_j)^2}{15\bar{e}^2}, \tag{5}$$

where e_i, e_j are the edge lengths and $\bar{e}$ is the mean edge length of the simplex. The number 15 used as normalization factor is the number of possible pairs of the six edges of a simplex. Clearly, it is $\mathbf{T} = 0$ for a perfect tetrahedron; for a quartoctahedron **T** is approximately 0.05, but the latter value is possible also for other (irregular) simplex shapes.

In a quartoctahedron there are five edges with the same length while the sixth edge is $\sqrt{2}$ times longer. Also this condition is one-to-one, i.e. a simplex with such edge lengths is definitely a quartoctahedron. Taking this into account, the measure of quartoctahedricity **Q** is defined as

$$\mathbf{Q} = \frac{(\sum_{i<j;i,j\neq m}(e_i - e_j)^2 + \sum_{i\neq m}(e_i - e_m/\sqrt{2})^2)}{15\bar{e}^2}, \tag{6}$$

see [23]. Here m is the index of the longest edge. It is $\mathbf{Q} = 0$ for a quartoctahedron and approximately 0.029 for a perfect tetrahedron; also this value is shared by other tetrahedra.

Figures 11 and 12 show the development of the distributions of **T** and **Q** with increasing density of hard sphere packings. With densification a development of two peaks can be observed in both distributions, which is already visible at $\phi = 0.62$ and becomes pronounced at $\phi = 0.67$. The first peak in the distribution of **T** corresponds to perfect tetrahedra and the second to quartoctahedra; for **Q** this is vice versa. In dense packings there are approximately two times more quartoctahedra than perfect tetrahedra, which is typical for systems with nearly fcc structure. Thus the measures **T** and **Q** are obviously sensitive to slight order variations in hard sphere packings and clearly recognize (nearly) crystalline structures.

A particularly elegant numerical characteristic in the given case of bimodality is the median. The median of a distribution is the point at which it is divided into two equal parts, with 50% of the values smaller and 50% larger. Figure 13 shows that the median of **Q** decreases with increasing ϕ, converging to zero, while the median of **T** decreases up to $\phi = 0.65$ and increases afterwards. This different behavior is closely related to the crystallization process: with growing density the degree of order increases in the packings and more and more nearly regular polyhedra appear. This leads first to decreasing values of **T** as well as of **Q**. With ongoing densification, however, obviously a development towards an fcc structure happens, where, as noted above, the number of quartoctahedra is twice the number of perfect tetrahedra. Thus the median is dominated by the quartoctahedra, which leads to the convergence towards zero for the **Q**-median and to increasing values for the **T**-median.

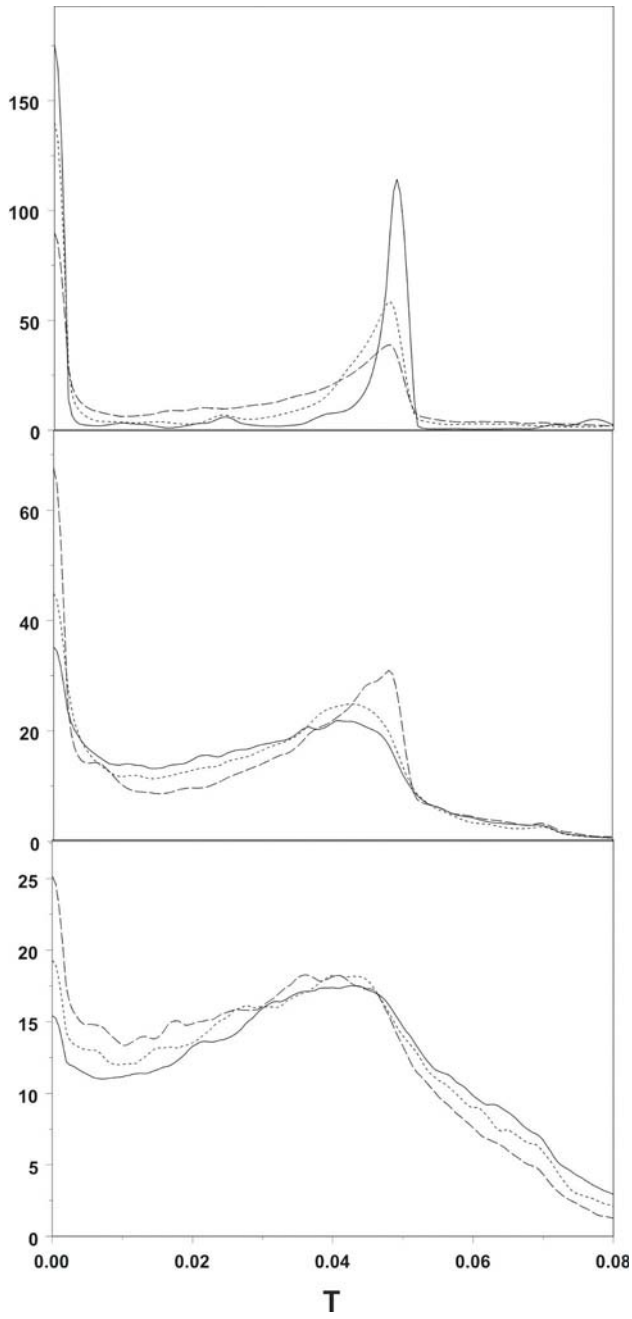

Fig. 11. Distributions of the tetrahedricity measure **T** for sphere packings with densities between 0.62 and 0.72: bottom — 0.62 (—), 0.63 (- - -), 0.64 (– – –); middle — 0.654 (—), 0.66 (- - -), 0.67 (– – –); top — 0.68 (– – –), 0.7 (- - -), 0.72 (—).

Note that instead of side lengths also angles [49] and procrustean shape characteristics [50] can be used.

Finally, in [51] the ratio T/Q of fractions of tetrahedral and quartoctahedral simplices is considered. This ratio is very sensitive to the packing density, in particular, to the appearance of crystalline nuclei in the packing. For models

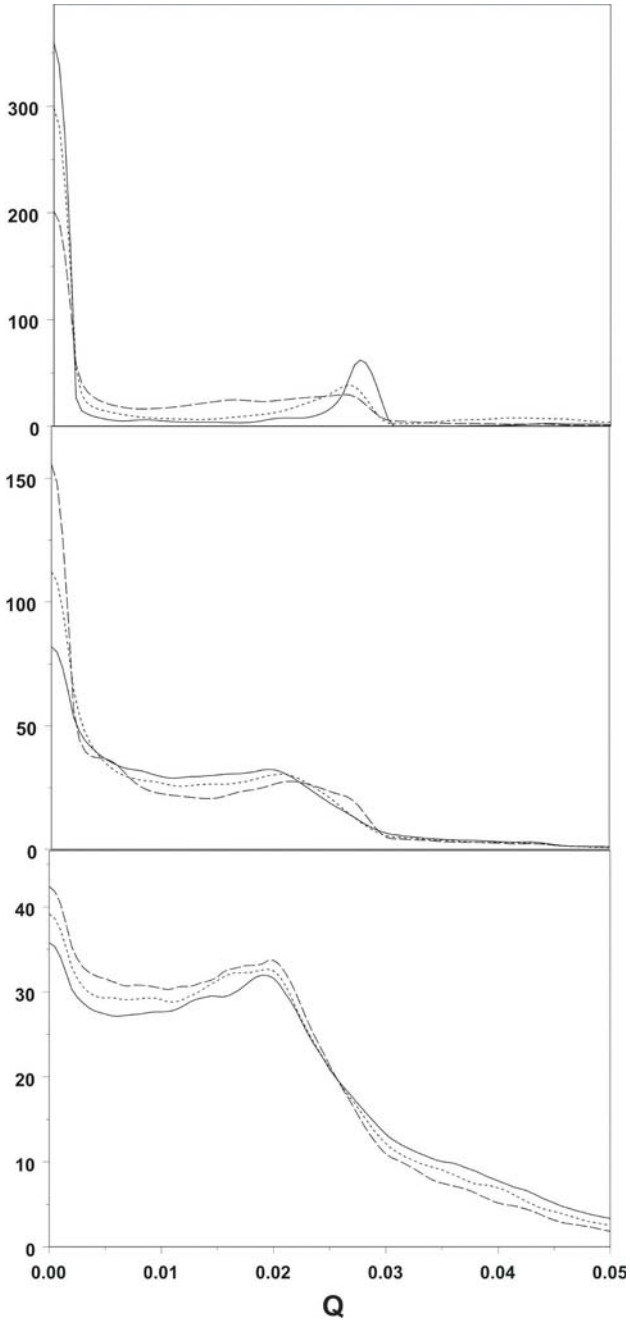

Fig. 12. Distributions of **Q** for sphere packings with densities between 0.62 and 0.72: bottom — 0.62 (—), 0.63 (- - -), 0.64 (– – –); middle — 0.654 (—), 0.66 (- - -), 0.67 (– – –); top — 0.68 (– – –), 0.7 (- - -), 0.72 (—).

generated by our algorithm the curve of T/Q via packing fraction shows a sharp peak at $\phi = 0.645 \pm 0.0015$. It was interpreted as a maximal value for the densest non-crystalline packing [51]. The packings obtained by the Lubachevsky-Stillinger algorithm behave quite similarly, which shows that our packings do not depend on the choice of one of these two algorithms. It also means that packings of maximal disorder might have a deep structural meaning.

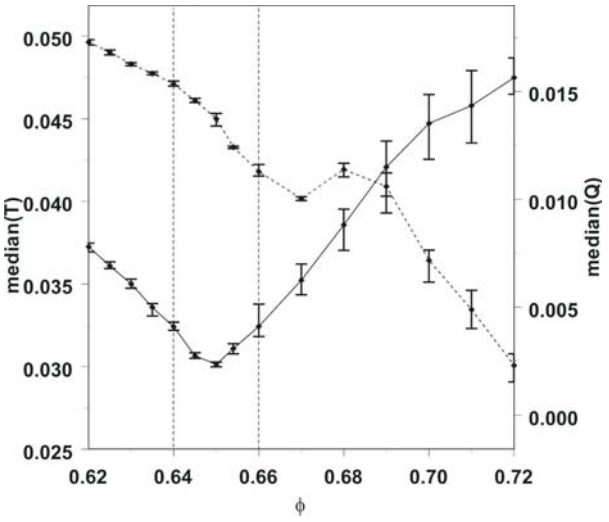

Fig. 13. Development of the medians of **T** (—) and **Q** (- - -) with densification of hard sphere packings. The minimum of the median curve for **T** indicates structural changes at ϕ between 0.64 and 0.66.

7 Conclusions

This paper analyzes the performance of various structure characteristics in the task of indicating structural changes in packings of hard spheres under densification. A set of such models of density ϕ from 0.62 to 0.72 is studied. Packings with ϕ lower than the known critical value 0.64 show a disordered (non-crystalline) behavior. Then, in the ϕ-interval between 0.64 and 0.66, fundamental structural changes happen: while at $\phi = 0.64$ there is still disorder, at 0.66 already considerable crystalline regions become clearly visible, and at 0.67 the packings present rather complete crystals although with numerous defects. For further increasing values of ϕ the crystal structure is improved continuously.

All considered order characteristics are able to recognize certain structural changes from disorder to crystalline structure. However, not all of them are sensitive enough to indicate different stages of crystallization. The Delaunay simplex shape measures **T** and **Q** turn out to be the most sensitive characteristics for this purpose. They recognize the beginning of crystallization better than the others because the simplices of given shapes present natural structure elements of the arising crystal structures (fcc and hcp).

The characteristics T as well as $\langle f \rangle$ and $\overline{Q}_{6,local}$ (and the corresponding variances) are of little value for the problem considered here, since they increase with increasing ϕ with only slowly varying slope. In contrast, the curves for $Q_{6,global}$ and $T_3(r)$ have sharp cusp points in the ϕ-interval 0.64–0.66, indicating massive appearance of crystals. Also the pair correlation function indicates structural changes for ϕ between 0.64 and 0.66. The first evidence of beginning crystallization (a peak at $r = \sqrt{2}$) appears at $\phi = 0.654$. However, the other specific crystalline peaks remain smoothed up to $\phi = 0.67$, after which they start to grow sharply.

We thank André Tscheschel for providing the program for the calculation of $T_3(r)$. The work was partly supported by Deutsche Forschungsgemeinschaft, Alexander von Humboldt Foundation, RFFI grant No. 05-03-32647 and YS INTAS grant No. 04-83-3865.

References

1. W.G. Hoover, F.H. Ree, J. Chem. Phys. **49**, 3609 (1968)
2. H. Reiss, A.D. Hammerich, J. Phys. Chem. **90**, 6252 (1986)
3. P. Richard, L. Oger, J.P. Troadec, A. Gervois, Phys. Rev. E **60**, 4551 (1999)
4. I. Volkov, M. Cieplak, J. Koplik, J.R. Banavar, Phys. Rev. E **66**, 061401 (2002)
5. S. Auer, D. Frenkel, J. Chem. Phys. **120**, 3015 (2004)
6. M. Robles, M.L. de Haro, A. Santos, S.B. Yuste, J. Chem. Phys. **108**, 1290 (1998)
7. J.D. Bernal, *Proceedings of the Royal Society of London*, Series A, Mathematical and Physical Sciences **280**, 299 (1964)
8. G. Mason, Nature **217**, 733 (1968)
9. G.D. Scott, D. Kilgour, Brit. J. Appl. Phys. (J. Phys. D) **2**, 863 (1969)
10. T. Aste, M. Saadatfar, T.J. Senden, Phys. Rev. E **71**, 061302 (2005)
11. A. van Blaaderen, P. Wiltzius, Science **270**, 1177 (1995)
12. W.S. Jodrey, E.M. Tory, Phys. Rev. A **32**, 2347 (1985)
13. A.S. Clarke, H. Jonsson, Phys. Rev. E **47**, 3975 (1993)
14. M. Rintoul, S. Torquato, Phys. Rev. E **58**, 532 (1998)
15. A. Bezrukov, M. Bargiel, D. Stoyan, Part. Part. Syst. Charact. **19**, 111 (2002)
16. J.D. Bernal, Nature **183**, 141 (1959)
17. J.L. Finney, Roy. Soc. London **319**, 479 (1970)
18. F.W. Starr, S. Sastry, J.F. Douglas, S.C. Glotzer, Phys. Rev. Lett. **89**, 125501 (2002)
19. J.L. Finney, J. Comp. Phys. **32**, 137 (1979)
20. B.N. Delaunay, *Proc. Math. Congr. Toronto*, 11–16 Aug. 1924 (Univ. of Toronto Press, 1928), pp. 695–700
21. N.N. Medvedev, Y.I. Naberukhin, J. Non-Chryst. Solids **94**, 402 (1987)
22. Y.I. Naberukhin, V.P. Voloshin, N.N. Medvedev, Molecular Physics **73**, 917 (1991)
23. N.N. Medvedev, *Voronoi-Delaunay method for non-crystalline structures* (SB Russian Academy of Science, Novosibirsk, 2000)
24. A. Okabe, B. Boots, K. Sugihara, S. Chiu, *Spatial tessellations-concepts and applications of Voronoi diagrams* (Wiley, 2000)
25. P.J. Steinhardt, D.R. Nelson, M. Ronchetti, Phys. Rev. B **28**, 784 (1983)
26. A. Mitus, H.Weber, D.Marx, Phys. Rev. E **55**, 6855 (1997)
27. T. Aste, J. Phys.: Condens. Matter **17**, S2361 (2005)
28. V. Luchnikov, A. Gervois, P. Richard, L. Oger, J.P. Troadec, J. Molecular Liquids **96, 97**, 185 (2002)
29. T.M. Truskett, S. Torquato, P.G. Debenedetti, Phys. Rev. E **62**, 993 (2000)
30. A.R. Kansal, S. Torquato, F.H. Stillinger, Phys. Rev. E **66** (2002)
31. R.M. Lynden-Bell, P.G. Debenedetti, J. Phys. Chem. B **109**, 6527 (2005)
32. K. Schladitz, A.J. Baddeley, Scand. J. Statist. **27**, 657 (2000)
33. N. Xu, J. Blawzdziewicz, C.S. O'Hern, Phys. Rev. E **71**, 061306 (2005)
34. F. Zamponi, e-print `arXiv:cond-matp.0604622` (2006)
35. A. Anikeenko, M. Gavrilova, N. Medvedev, LNCS **3480**, 816 (2005)
36. N.N. Medvedev, A. Bezrukov, D. Stoyan, J. Stuct. Chem. **45**, 24 (2004)
37. J. Moscinski, M. Bargiel, Computer Phys. Comm. **64**, 183 (1991)
38. W.S. Jodrey, E.M. Tory, J. Simulation **32**, 1 (1979)
39. M. Skoge, A. Donev, F.H. Stillinger, S. Torquato (2006); `http://atom.princeton.edu/Packing/C++/`
40. T.M. Truskett, S. Torquato, P.G. Debenedetti, Phys. Rev. E **62**, 993 (2000)
41. P.R. ten Wolde, M.J. Ruiz-Montero, D. Frenkel, Phys. Rev. Lett. **75**, 2714 (1995)
42. P.R. ten Wolde, M.J. Ruiz-Montero, D. Frenkel, J. Chem. Phys. **104**, 9932 (1996)
43. S. Torquato, T.M. Truskett, P.G. Debenedetti, Phys. Rev. Lett. **84**, 2064 (2000)
44. S. Torquato, *Random heterogeneous materials* (Springer, New York, 2002)
45. N.N. Medvedev, A. Geiger, W. Brostow, J. Chem. Phys. **93**, 8337 (1990)
46. A. Gervois, L. Oger, P. Richard, J.P. Troadec, International Conference on Computational Science (3), 95 (2002)
47. T.M. Truskett, S. Torquato, S. Sastry, P.G. Debenedetti, F.H. Stillinger, Phys. Rev. E **58**, 3083 (1998)
48. A.V. Anikeenko, M.L. Gavrilova, N.N. Medvedev, Jpn J. Indust. Appl. Math **22**, 151 (2005)
49. T. Aste, Phys. Rev. Lett. **96**, 018002 (2006)
50. A.V. Anikeenko, M.L. Gavrilova, N.N. Medvedev, *Proceedings of ISVD*, 2–5 July 2006, Banff, Canada (in press)
51. A.V. Anikeenko, N.N. Medvedev, A. Elsner, K. Lochmann, D. Stoyan, *Conference proceedings of ISVD*, 2–5 July 2006, Banff, Canada (in press)